Artificial Intelligence in Medicine (2008) **43**, 207—222

ELSEVIER

ARTIFICIAL INTELLIGENCE IN MEDICINE

http://www.intl.elsevierhealth.com/journals/aiim

Ovarian cancer diagnosis with complementary learning fuzzy neural network

Tuan Zea Tan [a], Chai Quek [a,*], Geok See Ng [a], Khalil Razvi [b]

[a] *Centre for Computational Intelligence, School of Computer Engineering, Nanyang Technological University, Block N4, #2A-32, Nanyang Avenue, Singapore 639798, Singapore*
[b] *Department of Obstetric and Gynaecology, Southend University Hospital NHS Foundation Trust, Prittlewell Chase, Westcliff-on-Sea, Essex SS0 0RY, UK*

Received 22 November 2006; received in revised form 15 April 2008; accepted 15 April 2008

KEYWORDS
Complementary learning;
Ovarian cancer diagnosis decision support;
Proteomics diagnosis;
Haemostasis blood assay diagnosis;
DNA micro-array diagnosis

Summary

Objective: Early detection is paramount to reduce the high death rate of ovarian cancer. Unfortunately, current detection tool is not sensitive. New techniques such as deoxyribonucleic acid (DNA) micro-array and proteomics data are difficult to analyze due to high dimensionality, whereas conventional methods such as blood test are neither sensitive nor specific.
Methods: Thus, a functional model of human pattern recognition known as complementary learning fuzzy neural network (CLFNN) is proposed to aid existing diagnosis methods. In contrast to conventional computational intelligence methods, CLFNN exploits the lateral inhibition between positive and negative samples. Moreover, it is equipped with autonomous rule generation facility. An example named fuzzy adaptive learning control network with another adaptive resonance theory (FALCON-AART) is used to illustrate the performance of CLFNN.
Results: The confluence of CLFNN-micro-array, CLFNN-blood test, and CLFNN-proteomics demonstrate good sensitivity and specificity in the experiments. The diagnosis decision is accurate and consistent. CLFNN also outperforms most of the conventional methods.
Conclusions: This research work demonstrates that the confluence of CLFNN-DNA micro-array, CLFNN-blood tests, and CLFNN-proteomic test improves the diagnosis accuracy with higher consistency. CLFNN exhibits good performance in ovarian cancer diagnosis in general. Thus, CLFNN is a promising tool for clinical decision support.

1. Introduction

Ovarian cancer accounts for 4% of all cancers among American and Canadian women, and ranks fourth as a cause of their deaths from cancer [1]. This high

* Corresponding author. Tel.: +65 6790 4926; fax: +65 6790 6559.
E-mail address: ashcquek@ntu.edu.sg (C. Quek).

0933-3657/$ — see front matter © 2008 Elsevier B.V. All rights reserved.
doi:10.1016/j.artmed.2008.04.003

death rate is due to the fact that almost 70% of women with ovarian cancer remained undiagnosed until the disease has advanced to Stage III or IV. To alleviate the situation, greater effort has to be focussed on the early detection of ovarian cancer since the survival rate is significantly higher if the disease is diagnosed at an early stage [2]. However, early detection of ovarian cancer is non-trivial. It is recorded that 13–21% of women who underwent surgery were found to be malignant [3]. Even annual routine gynaecologic and pelvic examinations have only detected 3% of the early stage ovarian cancer cases, and 10% of Stages I–IV cancer [4]. This highlights the difficulty of the task at stake, and the high false positive rate of present ovarian cancer diagnosis techniques.

Bimanual pelvic examination, sonography and tumour marker are some common modalities for ovarian cancer diagnosis. The reported accuracies of these techniques are summarized in Table 1. Sensitivity refers to the ratio of correctly identified malignant cases to the total population of malignant disease, whereas specificity is the ratio of correctly identified benign cases to the total benign popula-

Table 1 Ovarian cancer diagnosis modalities

Modality	Sensitivity (%)	Specificity (%)	Reference
Bimanual pelvic examination	26–67	94	[7,8]
Surgical procedure			
Pap smear	10–30	Not available	[6]
Imaging			
Transabdominal ultrasonography (TAS)	50–100	98	[5–8]
Transvaginal ultrasonography (TVS)	69–100	56–97	[7,9–12]
TVS & colour Doppler imaging (CDI)	50–100	46–100	[7,9–10,13,14]
Power Doppler (with end diastolic velocity distribution slope parameter)	91–97	90–100	[15]
Pulsed Doppler (with time averaged maximum velocity parameter)	89	81	[16]
Impedance/spectra/colour Doppler (with resistive index)	58–100	83–99	[13]
Colour Doppler (with pulsatility Index)	93	60	[13]
Power Doppler (with pulsatility index)	87	92–96	[13]
TVS & power Doppler (colour Doppler energy)	100	83	[9]
TVS & morphology index (MI)	≈100	99	[7]
TAS & CA-125	58–79	100	[6]
TVS & CA-125	94–97	91–100	[11]
TVS & MI & CDI	≈100	97	[7]
3D sonography	74	[14]	
3D power Doppler	54–95	99	[13,14]
3D sonography & 3D power Doppler	98–100	75	[13,14]
Computed tomography (CT)	47–100	79–93	[5,12,14,18,19]
CT with replicated reading	93–94	79–85	[20]
Positron emission tomography (PET)	10–100	40–100	[18,19]
2-Fluoro-2-deoxy-D-glucose & PET (FDG-PET)	10–88	42–100	[18]
PET-CT	62–73	40	[18,19]
Immunoscintigraphy	50–92	57–75	[17]
Magnetic resonance imaging (MRI)	81–100	88–100	[5,8,12,17]
MRI & immunoscintigraphy	89		[17]
Tumour marker			
CA-125	29–100	58–95	[6,7,11,21–23]
CA-125 & OVX1 antibody	80	91	[24]
CA-125 & TPS	81	82	[25]
Cancer-associated serum antigen	58	96	[25]
Platelet counts	59–77	60–65	[26]
Risk of malignancy index (RMI)	88	74	[22]
Carcinoembryonic antigen (CEA)	60	64	[21]
Oligonucleotide micro-array analysis	92	100	[27]
DNA sequence analysis	82	100	[27]

tion. In Table 1, sensitivity and specificity are estimated from the reported accuracies in tumour classification, malignant detection on pre- and post-menopausal patient.

dFrom Table 1, a large repertoire of ovarian screening techniques implies the difficulty associated with the ovarian cancer diagnosis task. Although most of the techniques appeared attractive, their accuracies are inconsistent. Every technique has its limitations. For example, the pelvic examination is the simplest way to discover ovarian cancer but it is unable to detect ovarian tumour at an early stage [5,6]. Surgical procedure like Pap smear, on the other hand, has very low sensitivity [6]. As for medical imaging modalities, they are inconsistent and highly dependent on the skill of the imaging technicians/operators. Hence, medical imaging diagnosis is subjective and error-prone [11,12,18].

Another modality is blood assay such as cancer antigen-125 (CA-125), albeit blood assay sensitivity is claimed to be low [5,21,25]. Furthermore, CA-125 becomes unreliable if the woman is pregnant [28]. Apart from that, new microbiology techniques such as deoxyribonucleic acid (DNA) micro-array and proteomics have emerged in recent years. Despite DNA micro-array and proteomics holding promising results for cancer diagnosis [29], both technologies are high dimensional and consequently the analysis becomes time-consuming [30]. Together with the lack of knowledge on the pre-cancer syndrome of ovarian cancer, the limited ovarian cancer micro-array and proteomics samples have hindered the progress of DNA micro-array and proteomics. In short, none of the modalities has sufficient sensitivity and specificity when used as a standalone tool [1], resulting in the difficulty of ovarian cancer diagnosis as well as the limitation of current screening tool. The high false positive rate not only produces suboptimal patient outcome, at the same time, it also incurred higher cost to both physician and patient. Thus, many have proposed to aid the ovarian cancer diagnosis using computational intelligence tools. A plethora of methods have been proposed to assist in fighting ovarian cancer, as summarized in Table 2.

As shown in Table 2, computational intelligence significantly enhances the diagnosis accuracy. These clinical decision support systems (CDSSs) reduced the inconsistency in medical decision. However, most of the adopted techniques have their shortcomings; they are namely: (1) not comprehensible—no facility for interpretation; (2) time-consuming—manual rule construction. Furthermore, most of the systems are based on either positive or neutral learning of cases and do not consider the contribution of negative classes. Consequently, these CDSS were unable to gain trust from physicians. Thus, complementary learning fuzzy neural network (CLFNN) is proposed. With complementary learning, the system learns from positive and negative examples. As a result, CLFNN generates positive and negative rules, which provides a closer representation of the problem. At the same time, CLFNN is capable of producing relatively superior classification performance because of the *lateral inhibition* feature existing between the positive and negative fuzzy rule-bases. In other words, a positive sample (malignant case) will concurrently activate the positive rules and inhibit the negative rules when presented to the system, hence leading to a positive conclusion. This minimizes the confusion in the inference process and produces relatively good classification performance. Apart from providing fuzzy rules to improve its comprehensibility, CLFNN also offers reasoning process that is closely akin to that performed by humans. Hence, CLFNN is more comprehensible in comparison to conventional methods. In this study, a CLFNN named fuzzy adaptive learning control network with another adaptive resonance theory (FALCON-AART) [43] is described to illustrate the feasibility of using CLFNN as an effective ovarian cancer CDSS.

This paper is organized as follows: Section 2 states the datasets used in this study, and briefly describe the features of CLFNN. Section 2 also covers the experimental setup. Section 3 describes the experimental results and analyses. Section 4 concludes the paper.

2. Methods and material

2.1. Dataset

Three datasets are used in this work. They are described in the following sections.

2.1.1. Micro-array gene expression

The first dataset is the micro-array gene expression for ovarian cancer diagnosis. The ovarian cancer dataset [44] consists of 30 samples obtained from ovarian tumours and 24 normal samples. Each of these samples comprises 1536 features. Class distribution of this ovarian cancer dataset is as follows:

- 24 samples of normal ovarian tumour.
- 1 sample of Stage I mucinous ovarian tumour.
- 24 samples of Stage III serous ovarian tumour.
- 5 samples of Stage IV serous ovarian tumour.

2.1.2. Blood assays

Another dataset is the ovarian cancer diagnosis based on blood tests, collected from Singapore National University Hospital (NUH). The dataset

Table 2 Reported accuracy on computer-aided ovarian diagnosis or prognosis

Medical inputs/modalities	Computational intelligence tool	Accuracy (%)	Training/ sample size
Ovarian cancer risk factors [22,31]	Bayesian network	93	225/300
	Naïve Bayesian	93	
	Artificial neural network	95	
	Logistic regression	90	
CA-125 II & CA-72-4 & CA-15-3 & lipid-associated sialic acid [23]	Multilayer perceptron	90	174/429
Patient data [32]	Genetic algorithm	80	Not mentioned
	Fuzzy genetic algorithm	78	
	Fuzzy logic system	70	
	Fuzzy logic + genetic algorithm	78	
	Genetic programming (logical rules)	84	
	Genetic programming (algebraic rules)	81	
	Multilayer perceptron	59	
	Multilinear regression	41	
Laparotomy data [33]	Multilayer perceptron	85	166/242
	Logistic regression	68	
	Linear regression	73	
Blood tests [34]	Multilayer perceptron	93	35/50
Patient history & ultrasonography measurements & colour Doppler imaging measurements & blood serum marker levels [35]	Bayesian network	62	Not mentioned
Magnetic resonance images [36]	Linear discriminant analysis	97	Not mentioned
Patient history [37]	Support vector machine	81	10-fold cross-validation, 199
Gene expression profile [38]	*k*-Nearest neighbour	71	Leave-one-out, 32
	CAST	43	
	Support vector machine	68	
	AdaBoosting	89	
Proteomic serum mass spectra [39]	Ensemble of 51 artificial neural network	91	100/215
Proteomics ovarian cancer serum mass spectra [40]	Genetic algorithms and Kohonen clustering	97	137/253
Proteomic spectrum [41]	Genetic algorithm	99	Not mentioned
Thermogram [42]	CLFNN	94	26/78

was collected over a period of 5 years from the NUH Department of Oncology and Gynaecology; consisting of 172 patients diagnosed using several blood tests. The class distribution is as follows:

- 23 samples of normal patient.
- 78 samples of benign cyst patient.
- 10 samples of borderline or proliferating tumour patient.
- 19 samples of Stages I and II patient.
- 42 samples of Stages III and IV patient.

Each diagnosed case is associated with the patient's profile, blood composition and some common blood test such as CA-125, cancer-associated serum antigen (CASA), etc. All features of the dataset are listed in Table 3.

2.1.3. Proteomic spectra

The third dataset [40] is the proteomic spectra generated by the Protein Biology System 2 surface-enhanced laser desorption/ionization-time of flight (SELDI-ToF) mass spectrometer. It contains 253 instances, each with 15,154 intensity of molecular mass per charge ratio. The class distribution is as follows:

- 91 samples of normal patient.
- 162 samples of ovarian cancer patient.

Table 3 List of ovarian features

x_1: age	x_{16}: D-dimer
x_2: packed cell volume (PCV)	x_{17}: tissue plasminogen activator (tPA) activity
x_3: hemoglobin (Hgb)	x_{18}: tPA antigen
x_4: β-Thromboglobulin (TG)	x_{19}: urokinase-like plasminogen activator (uPA) activity
x_5: reaction time of thrombelastography (TEG-r)	x_{20}: uPA antigen
x_6: coagulation time of TEG (TEG-K)	x_{21}: uPA receptor
x_7: maximum amplitude of TEG (TEG-MA)	x_{22}: PA inhibitor 1 (PAI-1) activity
x_8: fibrinogen	x_{23}: PAI-1 antigen
x_9: factor VII	x_{24}: PAI-2 antigen
x_{10}: von Willebrand-factor (VWF)	x_{25}: protein C antigen
x_{11}: thrombin–antithrombin complex (T/AT)	x_{26}: protein S antigen
x_{12}: prothrombin fragment 1 & 2 (F1 + 2)	x_{27}: cancer antigen-125 (CA-125)
x_{13}: antithrombin III (A-TH3) activity	x_{28}: cancer-associated serum antigen (CASA)
x_{14}: A-TH3 antigen	x_{29}: tissue factor pathway inhibitor (TFPI)
x_{15}: plasminogen	x_{30}: blood platelet

2.2. FALCON-AART

FALCON-AART belongs to the class of CLFNN. In contrast to conventional methods, CLFNN exploits positive and negative learning, as well as the lateral inhibition between these two classes. CLFNN has the following three characteristics:

1. Learning from positive and negative samples.
2. Segregation of positive and negative knowledge.
3. Exploitation of lateral inhibition between positive and negative classes.

Formally, complementary learning can be described as follows:

Given a universe of discourse **U** consisting of T elements, $\mathbf{U} = \{x^1, \ldots, x^t, \ldots, x^T\}$, a fuzzy set $\mathbf{A}_C$ representing a particular concept C, the elements in **U** will have unity membership if it belongs to the concept C (see Eq. (1)):

$$\mu_{\mathbf{A}_C}(x) = \begin{cases} 1 & \text{if } SM(x, \mathbf{A}_C) \geq \rho \\ 0 & \text{otherwise} \end{cases} \quad (1)$$

where SM(·) is a function for computing the similarity measure between the input to the reasoning system and the fuzzy set $\mathbf{A}_C$; and ρ is a predefined threshold. Similarly, elements that do not belong to concept C will have unity membership function for the concept $\neg C$. This is described in Eq. (2):

$$\mu_{\mathbf{A}_{\neg C}}(x) = \begin{cases} 1 & \text{if } SM(x, \mathbf{A}_{\neg C}) \geq \rho \\ 0 & \text{otherwise} \end{cases} \quad (2)$$

Through the lateral inhibition property, whenever a positive sample is presented to the system, the positive sample activates the positive rules and concurrently inhibits the negative rules, which leads to positive output of the system. Complementary learning therefore is believed to improve the system in pattern recognition.

FALCON-AART autonomously generates fuzzy rules in the form described by Eq. (3):

IF x_1 is **A** and x_2 is **B**, **THEN** y_1 is **C** and y_2 is **D** (3)

The fuzzy rule in Eq. (3) is an example of a system with two inputs and two outputs. It consists of five elements:

1. Input linguistic variables (x_1, x_2).
2. Input linguistic terms (**A**, **B**). This represents fuzzy entities such as tall, short, thin, fat, etc. FALCON-AART represents input linguistic terms with trapezoidal membership function.
3. If–Then rule: links the antecedent part (i.e. input linguistic variables and terms as above) with the consequent part (i.e. output linguistic variables and terms as below).
4. Output linguistic variables (y_1, y_2).
5. Output linguistic terms (**C**, **D**).

FALCON-AART has five layers that are mapped into the elements of the fuzzy rule (see Fig. 1).

Prior to the commencement of training, FALCON-AART has only the input and output layers. As training progresses, it automatically constructs its hidden layer using the modified Fuzzy ART algorithm [43]. An adaptive and gradually decreasing learning constant is applied to the algorithm such that structural learning becomes a function of time. With this, FALCON-AART is able to alleviate the stability-plasticity dilemma as well as to avoid the problem of generating non-representative or redundant clusters. It dynamically partitions the input and output spaces into trapezoidal fuzzy clusters, and subsequently these clusters are fine-tuned using the adaptive back-propagation algorithm. The tuning is performed on the slope as well as the kernel of the fuzzy sets. When new training patterns are presented, if they

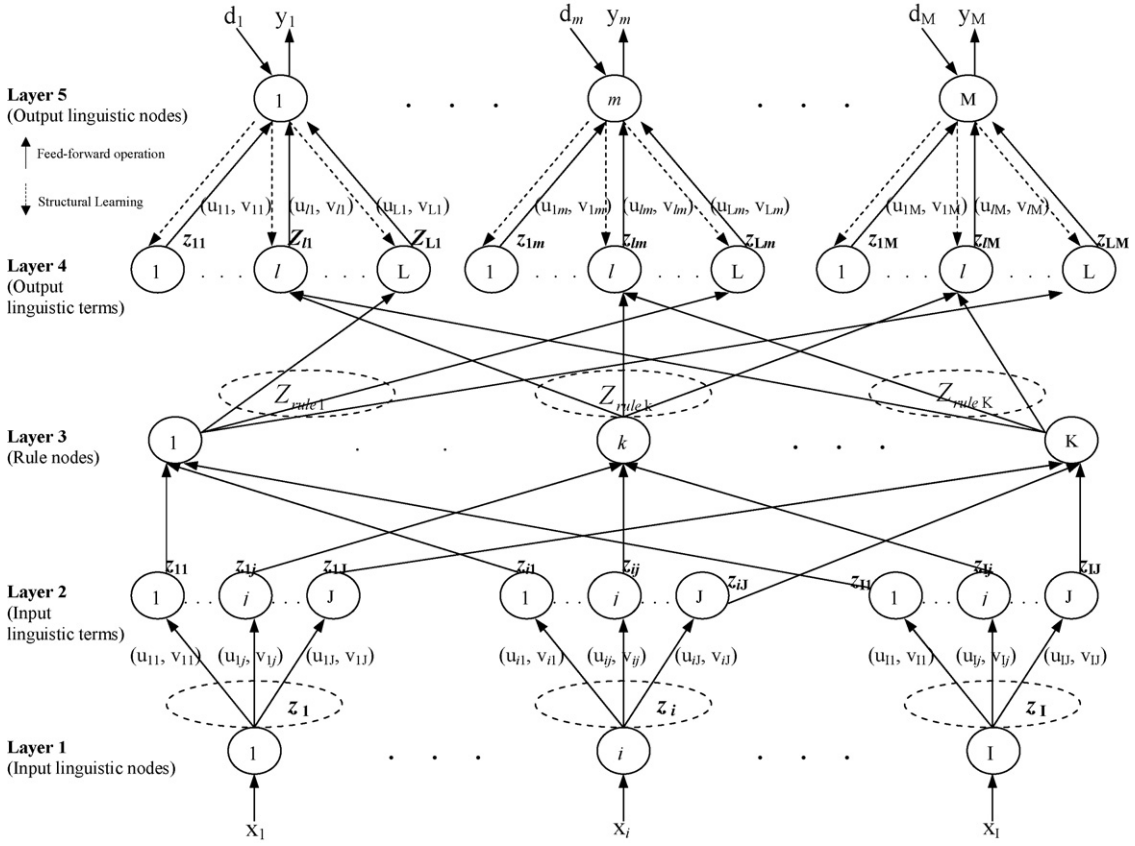

Figure 1 Architecture of FALCON-AART.

are sufficiently similar to the stored cluster, the stored cluster will resonate. The resonant cluster will then expand to incorporate these patterns using the structural learning algorithm. Training terminates when the mean square errors between two epochs are sufficiently equal. The inference process of FALCON-AART is summarized as follows.

Let $\mathbf{x} = (x_1, \ldots, x_i, \ldots, x_I)$ denotes the input, where $i \in [1, I]$ is the index to the input. Fuzzy sets **A** and **B** are the input and output fuzzy sets, respectively. A fuzzy set **A** is described by its membership function, denoted as $\mu_{\mathbf{A}}(x)$.

Step 1 *Input fuzzification*: input $\mathbf{x}^t = (x_1^t, x_2^t, \ldots, x_I^t)$ is fuzzified to $\overline{\mathbf{x}^t} = (\overline{x_1^t}, \overline{x_2^t}, \ldots, \overline{x_I^t})$ before feeding into the system.

Step 2 *Antecedent matching*: fuzzified input fuzzy sets are compared with their corresponding rule antecedents. Subsequently, the similarity measure (SM) is computed using Eq. (4):

$$\begin{aligned} \mathrm{SM} &= \mu_{\overline{x_i^t} \cap \mathbf{A}_{ij}}(x_i^t) \\ &= \overline{x_i^t} \cap \mathbf{A}_{ij} \\ &= \mu_{\overline{x_i^t}}(x_i^t) * \mu_{\mathbf{A}_{ij}}(x_i^t) \end{aligned} \tag{4}$$

where * is the *t*-norm operation. Since $\overline{x_i^t}$ is a fuzzy singleton, Eq. (4) can be simplified to Eq. (5):

$$\begin{aligned} \mathrm{SM} &= \mu_{\overline{x_i^t}}(x_i^t) * \mu_{\mathbf{A}_{ij}}(x_i^t) \\ &= 1 * \mu_{\mathbf{A}_{ij}}(x_i^t) \\ &= \mu_{\mathbf{A}_{ij}}(x_i^t) \end{aligned} \tag{5}$$

Step 3 *Rule fulfilment*: in this step, the overall similarity measure (OSM) between the fuzzified inputs and rule antecedents are computed using Eq. (6):

$$\mathrm{OSM}_{\mathrm{rule}\,k} = \frac{1}{I} \sum_{i}^{I} \mathrm{SM}_{ik} \tag{6}$$

where SM_{ik} is the similarity measure of the *i*th antecedent of rule *k*, and *I* is the input dimension.

Step 4 *Consequent derivation*: the consequents of the fired rules are derived based on the rules' OSM, as shown in Eq. (7):

$$\mu_{\overline{\mathbf{B}_{(lm)_k}}}(y_m) = \mu_{\mathbf{B}_{(lm)_k}}(y_m) \times z_{\mathrm{rule}\,k} \tag{7}$$

There may be more than one rule that is connected to a consequent. Hence, the final

inferred consequent derived is the aggregation of the different consequents inferred using different rules. The final inferred consequent is described in Eq. (8):

$$\begin{aligned}\overline{\mathbf{B}_{lm}} &= f[\overline{\mathbf{B}_{(lm)_k}}], \quad \text{where } f \text{ can be } \cap, \cup, \sum \\ &= \bigcup_{k\in\{1,2,\ldots,K\}} \overline{\mathbf{B}_{(lm)_k}}, \quad \text{choose } f \text{ to be } \cup \\ &= \max_{k\in\{1,2,\ldots,K\}} \{\mu_{\overline{\mathbf{B}_{(lm)_k}}}(y_m)\} \\ &= \max_{k\in\{1,2,\ldots,K\}} \{\mu_{\mathbf{B}_{(lm)_k}}(y_m) \times z_{\text{rule}\,k}\} \\ &= \max_{k\in\{1,2,\ldots,K\}} \{z_{\text{rule}\,k}\} \times \mu_{\mathbf{B}_{lm}}(y_m)\end{aligned} \tag{8}$$

Step 5 *Output defuzzification*: the final consequent derived from the output fuzzy sets are defuzzified to produce a crisp output. The center of area defuzzification is adopted and is described in Eq. (9):

$$y_m = \frac{\sum_{l=1}^{L} \mathrm{Kr}_{lm}\overline{\mathbf{B}_{lm}}}{\sum_{l=1}^{L} \overline{\mathbf{B}_{lm}}} \tag{9}$$

where Kr_{lm} is the kernel of fuzzy set $\mathbf{B}$.

Every FALCON-AART inference step has a one-to-one mapping to the human inference step, as shown in Table 4. This suggests that FALCON-AART has an inference process that is highly akin in a human.

2.3. Experimental setup

All the experiments are run on a system with an Intel Pentium IV 2 GHz processor, and 512 MB random access memory (RAM). Each sample of the dataset is divided into positive (malignant) and negative (benign and normal) classes. For every dataset, three stratified training and testing cross-validation sets are generated. The system is then trained and assessed using the training/testing sets. FALCON-AART is benchmarked against some popular tools [45], namely, naïve Bayesian (NB), radial basis function (RBF), adaptive network-based fuzzy inference system (ANFIS) [46], support vector machine (SVM), C4.5, *k*-nearest neighbour (kNN), and multilayer perceptron (MLP). The metrics used apart from classification accuracy are sensitivity and specificity which are described in Eqs. (10) and (11), respectively:

$$\text{sensitivity} = \frac{\text{number of positive samples correctly predicted}}{\text{total number of positive samples}} \tag{10}$$

$$\text{specificity} = \frac{\text{number of negative samples correctly predicted}}{\text{total number of negative samples}} \tag{11}$$

3. Experiments

3.1. DNA micro-array gene expression

Examination of the gene expression identified by DNA micro-array provides an important insight into the biology of ovarian cancer detection. However, gene expression obtained using DNA micro-array contains a large number of features (1536 genes for this dataset). It is impossible to employ all the features to classify. Even if it were possible, there will be redundant genes that may significantly contribute to classification error. Furthermore, classification using statistical method such as kNN and MLP cannot be quantitatively evaluated and interpreted in an intuitive and human-like manner. Owing to these issues, feature selection has to be undertaken to select the most relevant features prior to classification. For this dataset, sparse logistic regression [47] has been used to select the nine most relevant features. In order to illustrate that the improvement of the performance is due chiefly to the CLFNN and not the feature selection method, the experiments were repeated using another nine most relevant features selected by the SVM feature selection method [48]. Note that feature selection is only performed on the training set and not the testing set so that no bias is introduced. Each FALCON-AART is trained with different stratified set of

Table 4 Similarity of human and FALCON-AART inference

Human	FALCON-AART
Making observations	Feeding input to the system
Weighting the past experience or knowledge that describes the current situation	Computing overall similarity
Choosing the experience or knowledge that best reflects the current situation	Selecting maximally fired rule
Retrieving the actions of best matched past experience or knowledge	Determining the conclusion implied by the maximally fired rule
Acting out the actions	Output the conclusion

Table 5 Classification rate on ovarian cancer dataset (using sparse logistic regression)

Method	Sensitivity (%)	Specificity (%)	Accuracy (%)	Training time (s)	Number of rules
NB	33.30	96.70	68.50	0.01	NA
RBF	75.00	76.70	75.90	0.10	NA
ANFIS	75.00	76.70	75.90	1.80	9
SVM	58.30	56.70	57.40	0.80	NA
C4.5	79.20	70.00	74.00	0.60	4
kNN	70.80	86.70	79.60	0.02	NA
MLP	75.00	83.30	79.60	0.50	NA
FALCON-AART	62.50	100.00	81.30	0.06	5

NA: not available.

Table 6 Classification rate on ovarian cancer dataset (using SVM attribute selection)

Method	Sensitivity (%)	Specificity (%)	Accuracy (%)	Training time (s)	Number of rules
NB	87.50	93.30	90.70	0.01	NA
RBF	83.30	100.00	92.60	0.60	NA
ANFIS	83.30	96.70	90.70	1.60	12
SVM	33.30	100.00	70.40	0.10	NA
C4.5	87.50	93.30	90.70	0.30	3
Knn	83.30	96.70	90.70	0.02	NA
MLP	87.50	96.70	92.60	0.80	NA
FALCON-AART	90.00	91.70	90.70	0.50	10

NA: not available.

training and testing data (1/3 for training and 2/3 for testing). Classification performance of FALCON-AART is benchmarked against conventional methods and the averaged results are presented in Tables 5 and 6. The settings for the three-layer MLP are nine input nodes, eight hidden nodes, and one output node. Both hidden and output node activation functions are sigmoidal functions. It was trained using back propagation with momentum until the mean square error of training set reaches 10^{-8}. The SVM employed radial basis function as its kernel function and its C parameter was set at 2. The k value of kNN was chosen as 5. As for the ANFIS network, the membership function chosen is bell shape and the number of epoch is 100.

The most crucial advantage of FALCON-AART is its ability to provide reasoning for its computation. In contrast, MLP and kNN act as black boxes to the user, no rationale is provided to support their output. Table 7 lists the rules autonomously generated by FALCON-AART and C4.5. The linguistic terms such as 'low', 'medium' and 'high' are characterised by fuzzy sets that are dynamically constructed. Examples of the constructed fuzzy sets are shown in Fig. 2.

The number of rules generated by FALCON-AART is more than in a decision tree. This is because FALCON-AART is a CLFNN that learns from both positive and negative samples. Consequently, positive and negative rules are generated individually and they are segregated from each other. The rules generated by FALCON-AART are equipped with the capability to capture data uncertainty. In contrast to a decision tree, FALCON-AART is more tolerant to noise as small perturbation in the data would not generate a very different system. In addition, the rules in FALCON-AART allow the use of linguistic terms, giving the system greater expressive power. At the same time, it encapsulates unnecessary details from the user. From Table 7, the complexity of FALCON-AART rules is higher than those rules in a decision tree. A significant way to reduce the complexity of FALCON-AART is through careful feature selection prior to the training process. For illustration, when effective feature selection is performed prior to the FALCON-AART training, the complexity of the rules is significantly reduced. The rules generated by FALCON-AART are given in Table 8. Fig. 3 shows the graphical representation of the rules.

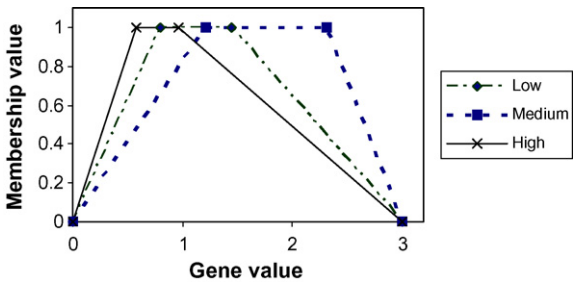

Figure 2 Fuzzy set constructed.

Table 7 Complementary rules generated by FALCON-AART and C4.5

	FALCON-AART	C4.5
Positive rule	**IF** gene1 is *very low* **AND** gene2 is *very low* **AND** gene3 is *medium* **AND** gene4 is *medium* **AND** gene5 is *high* **AND** gene6 is *marginal low* **AND** gene7 is *extremely low* **AND** gene8 is *low* **AND** gene9 is *very low* **THEN** Ovarian Cancer	**IF** gene5 $\leq$ 0.90 **AND** gene7 $\leq$ 9.95 **AND** gene6 $\leq$ 3.50 **THEN** Ovarian Cancer
Negative rule	**IF** gene1 is *marginal low* **AND** gene2 is *medium* **AND** gene3 is *marginal high* **AND** gene4 is *marginal high* **AND** gene5 is *marginal high* **AND** gene6 is *extremely high* **AND** gene7 is *low* **AND** gene8 is *high* **AND** gene9 is *low* **THEN** Normal	**IF** gene5 $>$ 0.90 **THEN** Normal

Table 8 Fuzzy rules with lower complexity

Rules	FALCON-AART
Positive rule	**IF** gene1 is *medium* **AND** gene2 is *marginal low* **AND** gene3 is *low* **Then** Ovarian Cancer
Negative rule	**IF** gene1 is *very low* **AND** gene2 is *low* **AND** gene3 is *very low* **Then** Normal

As shown in Table 8, the rules generated by FALCON-AART are now less complex and can be readily understood by the user. Unfortunately, there is trade off between interpretability and the performance of the system. With only three input features, the accuracy degrades from 92 to 70%, which is a 22% decline. Hence, one has to decide on the basis of the application to strike a balance between interpretability and performance. Graphical representation of the rules is given in Fig. 3. The fuzzy sets represent the input and output spaces. The range of the fuzzy sets describes the linguistic terms used in the rules, and captures the uncertainty in the data. Using these rules, it is shown that FALCON-AART possesses a human-like inference process, as illustrated by the flowchart in Fig. 4.

From Fig. 4, one can see that inference process of FALCON-AART is closely similar to human reasoning process, namely:

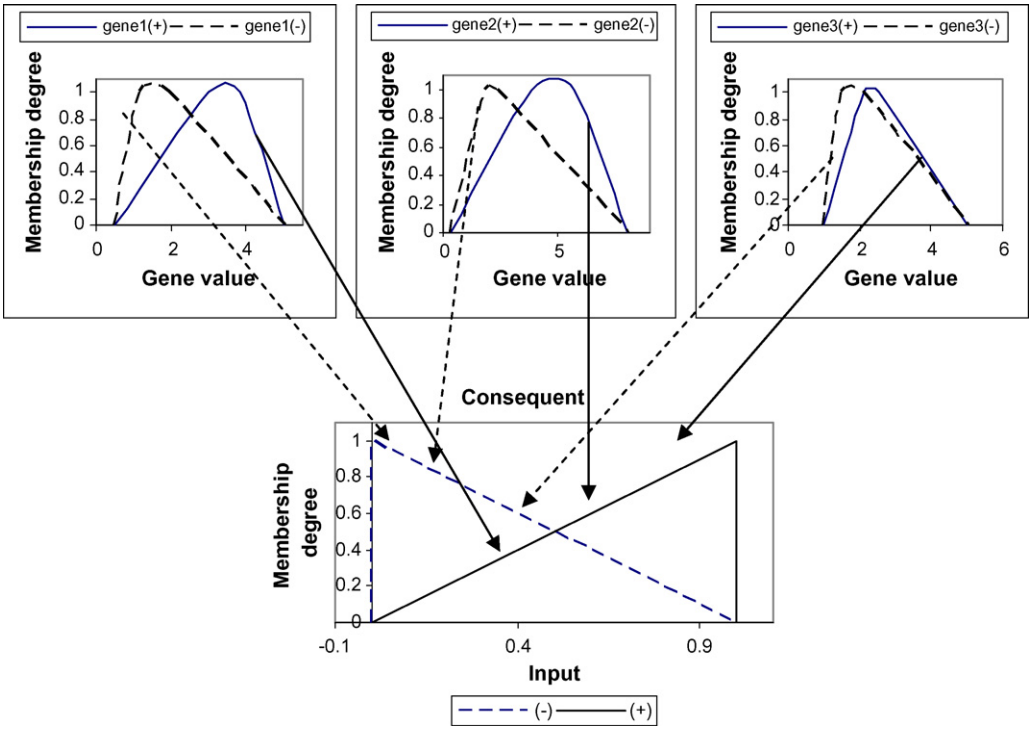

Figure 3 Graphical representation of fuzzy rules.

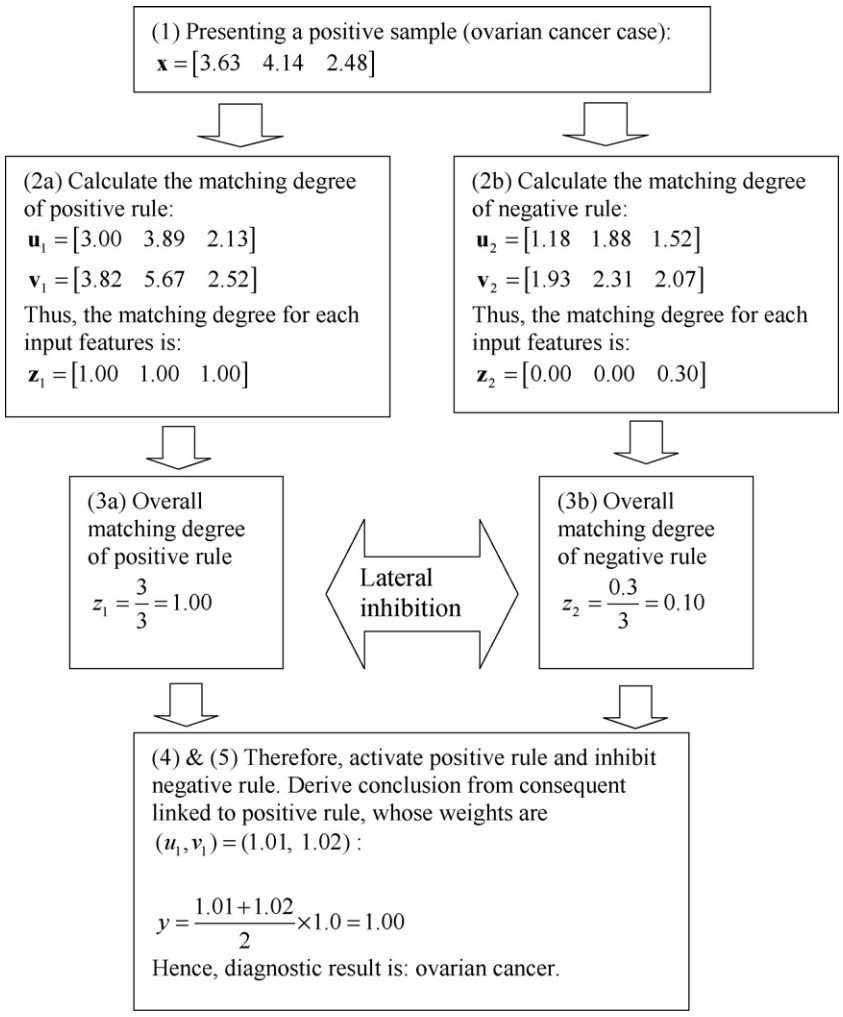

Figure 4 Inference process of FALCON-AART.

(1) Physician performs laboratory observation similarly FALCON-AART receives the data sample,
(2) Physician determines the matching degree of the current observation with his/her knowledge and experiences similarly FALCON-AART computes the matching degree of each rule,
(3) Physician selects the best-matched knowledge or experience similarly FALCON-AART activates the rule with the maximum overall matching degree,
(4) Physician evaluates the selected knowledge and gives his/her conclusion similarly FALCON-AART determines the consequent linked to the activated rule and derives the conclusion.

3.2. Blood test

In the blood assay dataset, not all blood test results are available for each case. Some cases have missing value in more than 10 features. Therefore, listwise deletion [49] is carried out. All cases with missing values are removed. Hence, the reduced set contains 62 normal and 45 ovarian cancer cases. The goal is to diagnose whether a patient has cancer or not based on the 30 blood test results. The averaged performance of the systems is shown in Table 9.

From Table 9, FALCON-AART outperforms most of the methods in ovarian cancer diagnosis. This shows that FALCON-AART is able to generalize the acquired/learnt knowledge well. The training time of FALCON-AART is quite close to the other conventional methods, and is acceptably fast. The number of rules generated by FALCON-AART is similar to those produced by the decision tree algorithm. However, it outperforms C4.5. These rules can be used to explain why and how FALCON-AART derives its decision. After careful validation, these fuzzy rules can be used to guide an inexperience physician. Fuzzy rule is better suited than crisp rule generated by the decision tree algorithm because fuzzy rule can handle uncertainty in the data while

Table 9 Result on ovarian cancer using blood test

Method	Sensitivity (%)	Specificity (%)	Accuracy (%)	Training time (s)	Number of rules
NB	73.20	60.00	67.60	0.02	NA
RBF	70.70	50.00	62.00	0.10	NA
ANFIS	92.00	55.00	74.30	2.60	10
SVM	100.00	33.30	60.00	0.05	NA
C4.5	100.00	50.00	78.90	20.00	4
kNN	87.80	43.30	69.00	0.01	NA
MLP	90.20	50.00	73.20	1.90	NA
FALCON-AART	95.00	57.00	78.90	0.50	5

Table 10 Different diagnostic rules

Fuzzy rule	Expert diagnostic rule	Crisp rule
IF *age* is young **AND** *blood platelet* is few **AND** PCV is high **AND** Hgb is medium **AND** TG is medium **AND** TEG-r is very fast **AND** TEG-K is medium **AND** TEG-MA is quite small **AND** *fibrinogen* is quite small **AND** *factor VII* is quite high **AND** T/AT is medium **AND** VWF is quite high **AND** *antithrombin activity* is marginal low **AND** *antithrombin antigen* is medium **AND** *plasminogen* is quite small **AND** D-*Dimer* is very low **AND** tPA *activity* is very high **AND** tPA *antigen* is very high **AND** uPA *activity* is high **AND** uPA *antigen* is very high **AND** uPA *receptor* is medium **AND** PAI-1 *activity* is marginal low **AND** F1 + 2 is quite low **AND** PAI-1 *antigen* is quite low **AND** PAI-2 *antigen* is quite low **AND** *Protein S antigen* is quite high, **THEN** Normal	**IF** CA-125 is less than 35 U/ml **THEN** Normal [28] **IF** F1 + 2 is about 1.4 nmol/l **THEN** Normal [50] **IF** T/AT is about 0.8—5.0 mg/l **THEN** Normal [51] **IF** D-Dimer is approximately 0.5 mg/ml **THEN** Normal [50]	**IF** *age* $<$ 37 **AND** *plasminogen* $\leq$ 104 **THEN** Normal

crisp rule cannot. Examples of fuzzy rule, expert diagnostic rule, and crisp rule are given in Table 10.

As shown in Table 10, FALCON-AART rule is highly similar to the diagnostic rule used by a physician. FALCON-AART not only has a human-like reasoning process, but also has the facility that allows physician to justify and evaluate its decision using familiar terms. Note that if the details are needed, the exact range of values mediated by the linguistic term can be extracted from FALCON-AART. In contrast to the crisp rule generated by a decision tree, the fuzzy rules generated by FALCON-AART can cater to uncertainty that may be present in the blood test results due to erroneous recording or measurement. Crisp rule generated by a decision tree is limited in its expressive power because it does not allow the application of linguistic hedges such as "about", "approximately", which are often found in expert diagnostic rule. On the contrary, FALCON-AART rule is more akin to an expert diagnostic rule, and has superior modelling capacity because it employs complementary learning by which rules are generated for each class. FALCON-AART also allows the use of linguistic hedges. Note that the linguistic terms such as "young", "few" and "high" are described by the fuzzy sets autonomously constructed by FALCON-AART. It encapsulates unnecessary details from the physician and hence, allows easier interpretation. An example of

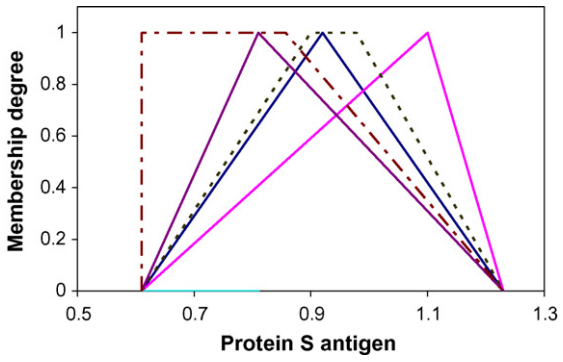

Figure 5 Subset of fuzzy set on protein S antigen.

the fuzzy set is shown in Fig. 5. The total overlapping region tells that this particular test is not useful for distinguishing the classes. Triangular fuzzy sets mediate the meaning of less uncertainty, whereas trapezoidal fuzzy sets capture more uncertainties present in the blood test.

Although the use of full input dimension for classification can reduce the chance of getting contradicting rules, it may render the rule non-readable due to the higher dimensionality. As interpretability of the system is paramount, especially for clinical decision support, efforts have to be put in to enhance the system comprehensibility. An established approach is to perform feature selection prior to the system training. The aim is to reduce the number of input dimension, and to trim off irrelevant blood test that is not a strong discriminating indicator for the different classes. Simpler rule can be generated with a reduced set of rules giving rise to clarity and potentially superior recognition performance. Four groups of training/testing set are generated; each containing the 10 most relevant features selected using *Monte Carlo* feature selection method [52]:

- G1: x_2, x_8, x_9, x_{10}, x_{11}, x_{12}, x_{14}, x_{17}, x_{27}, and x_{30}.
- G2: x_2, x_7, x_9, x_{11}, x_{17}, x_{18}, x_{21}, x_{22}, x_{29}, and x_{30}.
- G3: x_5, x_7, x_9, x_{11}, x_{12}, x_{15}, x_{23}, x_{24}, x_{25}, and x_{27}.
- G4: x_1, x_3, x_8, x_9, x_{11}, x_{14}, x_{16}, x_{23}, x_{24}, and x_{30}.

The results are listed in Table 11. The performance improves when the 10 most relevant features are used for classification. A mean accuracy of 91% can be attained. This suggests that blood tests CA-125, PA inhibitor 1, are important ovarian cancer indicators.

Apart from assisting in diagnosis, FALCON-AART can be used as a concept validation tool for hypotheses associated with ovarian cancer diagnosis. For example, it is known that effective classification of borderline and benign ovarian cancer is difficult [53], but there is no well-established support for this. Hence, one can conduct an experiment using FALCON-AART to classify borderline and benign ovarian cancer. To illustrate this, datasets G5—G7 that contain only borderline—benign, borderline—Stages I and II, and borderline—Stages III and IV data are created. The task is to identify the cases of borderline cancer from the other cases. The result is shown in Table 12. As can be seen in Table 12, it is relatively easier to distinguish cases of borderline cancer from other stages of ovarian cancer in contrast against benign cases. This provides supporting evidence to the conjecture that borderline cases are indeed difficult to be distinguished from benign cases.

Table 11 Result of ovarian cancer diagnosis using lesser features

Training/testing	Sensitivity (%)	Specificity (%)	Accuracy (%)
G1			
Benign	66.70	100.00	88.20
I & II	40.00	100.00	85.00
III & IV	100.00	100.00	100.00
Mean	68.90	100.00	91.10
G2			
Benign	100.00	90.90	94.10
I & II	40.00	100.00	85.00
III & IV	100.00	75.00	88.20
Mean	80.00	88.60	89.10
G3			
Border	20.00	100.00	93.00
Benign	60.70	84.60	72.20
I & II	14.30	100.00	88. 90
III & IV	94.10	81.10	85.20
Mean	47.30	91.40	84.80
G4			
Border	20.00	100.00	93.00
Benign	57.10	88.50	72.20
I & II	14.30	100.00	88. 90
III & IV	82.40	91. 90	88.90
Mean	43.50	95.10	85.80

3.3. Proteomic pattern

Proteomics is the study of protein. Since disease can occur due to gene and post-transcription mutation, and the fact that protein is the one that controls the cellular function, protein study provides different perspective in cancer research and could potentially revolutionize the conventional medical practice. The success of proteomics in other study has demonstrated that it is a promising tool for gynaecological cancers [30]. However, the analysis of the large number of proteins is difficult, and therefore requires effective bio-informatics tool. For this dataset, as there are 15,154 features, it is difficult to incorporate all features to train the system. It would incur enormous amount of time and would be very expensive. Hence, the top 50 most relevant features are extracted using the augmented variance ratio (AVR) [54], as described in Eq. (12):

$$\mathrm{AVR}(x) = \frac{S_b(x)}{(1/d)\sum_{i=1}^{d} S_i(x) / \min_{i \neq j} |\mu_i(x) - \mu_j(x)|} \tag{12}$$

where d is the number of classes, $S_i(x)$ is the within-class variance for ith class, $S_b(x)$ is the between-class variance, and $\mu_i(x)$ is the mean for ith class.

Table 12 Classification of borderline cancer from other cases

Set	Sensitivity (%)	Specificity (%)	Predict (%)	Number of rules	Training time (s)
G5 (border vs. benign)	0.00	100.00	93.30	14.00	2.00
G6 (border vs. I & II)	50.00	100.00	94.70	9.00	0.70
G7 (border vs. III & IV)	20.00	100.00	94.70	3.00	0.10

Since the AVR ignores the possible interactions between the features, SVM feature selection method [48] is applied to the top 50 most relevant features, taking into consideration the possible relationship between these features for feature ranking. As there is no systematic way of determining the optimal set of features, FALCON-AART is applied to this ovarian cancer diagnosis study of proteomic pattern using different number of features. The averaged accuracy versus the number of features is given in Fig. 6. It can be seen that the confluence of FALCON-AART and proteomics yields significant and promising performance. Even with only 1/3 of the samples used, an accuracy of 100% can be attainable. This shows that generalization capability of FALCON-AART, as well as the potential of complementing proteomic pattern analysis with CLFNN. From Fig. 6, 97.02% has been achieved with FALCON-AART when using only the most relevant gene. This shows that proteomic pattern analysis is indeed a very promising and effective tool for ovarian cancer diagnosis. Most of the conventional methods are able to achieve close to 100% accuracy using the same training and testing sets. Hence, only MLP and C4.5 are presented together with FALCON-AART in Fig. 6. As seen in Fig. 6, the proteomic features work differently under different methods. This affirms that there is no panacea that will work for all types of problems. A method perform well in one area may not perform well in another. The oscillation observed in the beginning for C4.5 suggests that some of the features may act as noise to the system. These irrelevant features affect the system performance. All in all, FALCON-AART offers

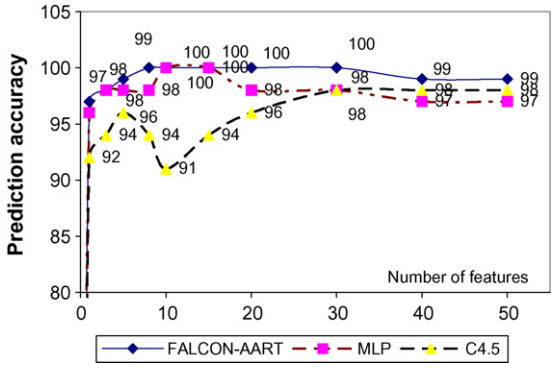

Figure 6 Accuracy vs. number of features.

the most consistent performance over different number of features, demonstrating that FALCON-AART is a competent system that is highly feasible for realizing CDSS.

4. Conclusion

FALCON-AART has demonstrated its superior capability as a CDSS for ovarian cancer diagnosis. Fast training, simple fuzzy rule generation, and superior accuracy are advantages exhibited by FALCON-AART in this study. Most significantly, FALCON-AART has the ability to generate complementary fuzzy rules for its reasoning process. These rules could potentially aid physicians in their analysis as well as their diagnostic decision process for ovarian cancer. FALCON-AART performs consistently with accuracies on par or superior to other conventional approaches used in the benchmark for the ovarian cancer diagnostic task. It automatically and judiciously constructs the complementary fuzzy rule knowledge from large dataset such as micro-array. It outperforms conventional artificial neural network and statistical methods in terms of accuracy. Furthermore, the FALCON-AART reasoning process is closely akin to the human reasoning process, which allows system analysis using familiar terms. Comparing the experimental results of FALCON-AART with those in Tables 1 and 2, it is shown that FALCON-AART indeed improves the accuracy of the diagnosis, providing a highly attractive alternative to other computational techniques for ovarian cancer detection. Moreover, it has enabled a more consistent performance in ovarian cancer detection with accurate decision support. FALCON-AART improves the system comprehensibility as well as the accuracy in ovarian cancer detection. The interpretability of the decision system can be further enhanced when the rules adhere to the set of interpretability criteria [55]. However, they are not considered in this work. Other related works that have been developed at the Centre for Computational Intelligence [56] that partially address this issue are [57,58] which employ rough set and Hebbian ordering in rule reduction. On the other hand, the attractive accuracy offered by the confluence of FALCON-AART — gene expression profile, and the confluence of FALCON-AART — proteomic pattern,

affirms the values of these tools in ovarian cancer diagnosis. In the future, FALCON-AART can be built based on other clinical ovarian cancer screening tools such as sonography, gene expression profile, and proteomic pattern. These CDSS can then complement each other in ovarian cancer diagnosis, and this multimodal diagnostic approach is believed to enhance the accuracy of ovarian cancer diagnosis. Also in this work, it is found that not all the blood tests are relevant to ovarian cancer diagnosis, as suggested by the experimental result of training/testing set G1—G4, where using the 10 most relevant blood tests boosts the classification accuracy. The proteomic method provides the most interesting result, confirming its huge potential in combating ovarian cancer. Alternatively, the different types of CLFNN such as genetic and hierarchical complementary learning [59—63] can also be used to form an ensemble system to complement each of the medical approach. Another improvement can be achieved by incorporating the concept of chance into the system [64] so as to enhance the interpretability of the CDSS. It has also been illustrated that FALCON-AART can be employed as a *concept validation* tools to validate clinical hypotheses or conjectures by adequate experimental settings. In this study, FALCON-AART was employed to support for the conjecture: borderline cases are difficult to be classified from benign cases. In the future, with the availability of data, it can be applied to validate other hypotheses or theories associated with ovarian cancer. For example, breast-feeding, age, race, obesity, number of ovulations, level of gonadotropins, carcinogens and gene deficiencies are risk factors for ovarian cancer [31].

References

[1] American Cancer Society. Cancer facts and figures. US: American Cancer Society; 2007.

[2] Jermal A, Murray T, Samuels A, Ghafoor A, Ward E, Thun MJ. Cancer statistic 2003. CA: Cancer Journal for Clinician 2003;13:5—26.

[3] NIH, NIH consensus conference. Ovarian cancer. Screening, treatment, and follow-up, NIH Consensus Developmental Panel on Ovarian Cancer. Journal of the American Medical Association 1995;273(6):491—7.

[4] Petignat P, Joris F, Faltin D. Importance of the general practitioner in the early detection of ovarian cancer. Gynecologic Oncology 2003;90:491—500.

[5] Kurtz AB, Tsimikas JV, Tempany CMC, Hamper UM, Arger PH, Bree RL, et al. Diagnosis and staging of ovarian cancer: comparative values of Doppler and conventional US, CT, and MR imaging correlated with surgery and histopathologic analysis—report of the radiology diagnostic oncology group. Radiology 1999;212:19—27.

[6] US Preventive Services Task Force. Guide to preventive services, 2nd ed., Washington, DC: US Department of Health and Human Services, Office of Disease Prevention and Health Promotion; 1996.

[7] Fiorica JV, Roberts WS. Screening for ovarian cancer. Cancer Control 1996;3(2):120—9.

[8] Low RN, Saleh F, Song SYT, Shiftan TA, Barone RM, Lacey CG, et al. Treated ovarian cancer: comparison of MR imaging with serum CA-125 level and physical examination—a longitudinal study. Radiology 1999;211:519—28.

[9] Guerriero S, Alcazar JL, Ajossa S, Lai MP, Errasti T, Mallarini G, et al. Comparison of conventional color Doppler imaging and power Doppler imaging for the diagnosis of ovarian cancer: results of a European study. Gynecologic Oncology 2001;83: 299—304.

[10] Jeong Y, Outwater EK, Kang HK. Imaging evaluation of ovarian masses. Radiographics 2000;20:1445—70.

[11] Kusnetzoff D, Gnochi D, Damonte C, Sananes C, Giaroli A, di Paolo G, et al. Differential diagnosis of pelvic masses: usefulness of CA125, transvaginal sonography and echo-Doppler. International Journal of Gynecology Cancer 1998;8(4):315—21.

[12] Loyer EM, Whitman GJ, Fenstermacher MJ. Imaging of ovarian carcinoma. International Journal of Gynecology Cancer 1999;9:351—61.

[13] Cohen LS, Escobar PF, Scharm C, Glimco B, Fishman DA. Three-dimensional power Doppler ultrasound improves the diagnostic accuracy for ovarian cancer prediction. Gynecologic Oncology 2001;82:40—8.

[14] Kurjak A, Kupesic S, Sparac V, Prka M, Bekavac I. The detection of stage I ovarian cancer by three-dimensional sonography and power Doppler. Gynecologic Oncology 2003;90:258—64.

[15] Shaharabany Y, Akselrod S, Tepper R. A sensitive new indicator for diagnostics of ovarian malignancy, based on the Doppler velocity spectrum. Ultrasound in Medicine & Biology 2004;30(3):295—302.

[16] Tailor A, Jurkovic D, Bourne TH, Natucci M, Collins WP, Campbell S. A comparison of intratumoural indices of blood flow velocity and impedance for the diagnosis of ovarian cancer. Ultrasound in Medicine and Biology 1996;22(7): 837—43.

[17] Low RN, Carter WD, Saleh F, Sigeti JS. Ovarian cancer: comparison of findings with perfluorocarbon-enhanced MR imaging, in-111-CYT-103 immunoscintigraphy and CT. Radiology 1995;195:391—400.

[18] Makhija S, Howden N, Edwards R, Kelley J, Townsend DW, Meltzer CC. Positron emission tomography/computed tomography imaging for the detection of recurrent ovarian and fallopian tube carcinoma: a retrospective review. Gynecologic Oncology 2002;85:53—8.

[19] Pannu HK, Cohade C, Bristow RE, Fishman EK, Wahl RL. PET-CT detection of abdominal recurrence of ovarian cancer: radiologic-surgical correlation. Abdominal Imaging 2004;39: 398—403.

[20] Fultz PJ, Jacobs CV, Hall WJ, Gottlieb R, Rubens D, Totterman SMS, et al. Ovarian cancer: comparison of observer performance for four methods of interpreting CT scans. Radiology 1999;212:401—10.

[21] Lapchenkov VI, Dudarev AL, Vinokurov VL, Yurkova LE, Barbanel Elu. Comparative evaluation of diagnostic significance of carbohydrate antigen CA125 and cancer-embryonal antigen in ovarian cancer. Vestnik Rentgenologii I Radiologii 1993;5:30—1 (in Russian).

[22] Timmerman D. Ultrasonography in the assessment of ovarian and tamoxifen-associated endometrial pathology. PhD dissertation. Leuven University Press; 1997.

[23] Zhang Z, Zhang H, Bast Jr RC. An application of artificial neural networks in ovarian cancer early detection. In: Amari

S-I, Lee Giles C, Gori M, Piuri V, editors. Proceedings of the IEEE international joint conference on neural networks, vol. 4. US: The Institute of Electrical and Electronics Engineers, Inc.; 2000. p. 107—12.
[24] Runowicz CD. Ovarian cancer screening. In: American College of Medical Genetic Foundation, Genetic susceptibility to breast and ovarian cancer: assessment, counseling and testing guidelines. New York State Department of Health; 1999.
[25] Sliutz G, Tempfer C, Kainz C, Mustafa G, Gitsch G, Koelbl H, et al. Tissue polypeptide specific antigen and cancer associated serum antigen in the follow-up of ovarian cancer. Anticancer Research 1995;15(3):1127—9.
[26] Bozkurt N, Yuce K, Basaran M, Kose F, Ayhan A. Correlation of platelet count with second-look laparotomy results and disease progression in patients with advanced epithelial ovarian cancer. Obstetric Gynecology 2004;103(1):82—5.
[27] Wen W, Bernstein L, Lescallett J, Beazer-Barclay Y, Sullivan-Halley J, White M, et al. Comparison of *TP53* mutations identified by oligonucleotide micro-array and conventional DNA sequence analysis. Cancer Research 2000;60:2716—22.
[28] The University of Iowa's Cancer Center. Tumour marker tests. University of Iowa; 2002 , available http://www.vh.org/adult/patient/cancercenter/tumormarker [accessed June 20, 2006].
[29] Yang ST. Micro-array application in medicine; 2002, available http://binfo.ym.edu.tw/styang/seminar/medicine/array_medicine.htm [accessed June 20, 2006].
[30] Kohn EC, Mills GB, Liotta L. Promising directions for the diagnosis and management of gynecological cancers. International Journal of Gynaecology Obstetric 2003;83(Suppl 1):203—9.
[31] Antal P, Verrelst H, Timmerman D, Moreau Y, Van Huffel S, De Moor B, et al. Bayesian networks in ovarian cancer diagnosis: potentials and limitations. In: Proceedings of 13th IEEE on computer-based medical systems. US: The Institute of Electricals and Electronics Engineers, Inc.; 2000. p. 103—8.
[32] Odusanya AA. Ovarian cancer prognosis and soft computing. In: Clark JW, McIntire LV, Ktonas PY, Mikos AG, Ghorbel FH, editors. Proceedings of the second joint EMBS/BMES conference, vol. 1. US: The Institute of Electricals and Electronics Engineers, Inc.; 2002. p. 60—1.
[33] Snow PB, Brandt JM, Larry Williams R. Neural network analysis of the prediction of cancer recurrence following debulking laparotomy and chemotherapy in Stages III and IV ovarian cancer. Molecular Urology 2001;5(4):171—4.
[34] Renz C, Rajapakse JC, Razvi K, Liang SKC. Ovarian cancer classification with missing data. In: Wang L, Rajapakse JC, Fukushima K, Lee SY, Yao X, editors. Proceedings of the ninth international conference on neural information processing, vol. 2. US: The Institute of Electricals and Electronics Engineers, Inc.; 2002. p. 809—13.
[35] Antal P, Fannes G, Timmerman D, Moreau Y, De Moor B. Using literature and data to learn Bayesian networks as clinical models of ovarian tumors. Artificial Intelligence in Medicine 2004;30:257—81.
[36] Wallace JC, Raaphorst GP, Somorjai RL, Ng CE, Fung FK, Senterman M, et al. Classification of ^{1}H MR spectra of biopsies from untreated and recurrent ovarian cancer using linear discriminant analysis. Magnetic Resonance in Medicine 1997;38(4):569—76.
[37] Kusy M. Application of SVM to ovarian cancer classification problem. In: Rutkowski L, et al., editors. Proceedings of the international conference on artificial intelligence and soft computing. Lecture Notes in Artificial Intelligence 3070. Berlin, Heidelberg: Springer-Verlag; 2004. p. 1020—25.
[38] Ben-Dor A, Bruhn L, Friedman N, Nachman I, Schummer M, Yakhini Z. Tissue classification with gene expression profiles. In: Shamir R, Miyano S, Istrail S, Pevzner P, Waterman M, editors. Proceedings of the fourth annual international conference on computational molecular biology. New York: ACM; 2000. p. 54—64.
[39] Loo L, Quinn J, Cordingley H, Roberts S, Hrebien L, Kam M. Classification of SELDI-ToF mass spectra of ovarian cancer serum samples using a proteomic pattern recognizer. In: Reisman S, Foulds R, Mantilla B, editors. Proceedings of IEEE 29th annual bioengineering conference. US: The Institute of Electricals and Electronics Engineers, Inc.; 2003. p. 130—1.
[40] Petricoin III EF, Ardekani AM, Hitt BA, Levine PJ, Fusaro VA, Steinberg SM, et al. Use of proteomic patterns in serum to identify ovarian cancer. Lancet 2002;359:572—7.
[41] Stevens EV, Liotta LA, Kohn EC. Proteomic analysis for early detection of ovarian cancer: a realistic approach? International Journal of Gynecology Cancer 2003;13(Suppl 2): 133—9.
[42] Tan TZ, Quek C, Ng GS, Ng EYK. A novel cognitive interpretation of breast cancer thermography with complementary learning fuzzy neural memory structure. Expert Systems with Applications 2007;33(3):652—66.
[43] Tan TZ, Quek C, Ng GS. Ovarian cancer diagnosis by hippocampus and neocortex-inspired learning memory structures. Neural Networks 2005;18(5/6):818—25.
[44] Schummer M, Ng W, Bumgarner R, Nelson P, Schummer B, Bednarski D, et al. Comparative hybridization of an array of 21,500 ovarian cDNAs for the discovery genes overexpressed in ovarian carcinomas. Gene 1999;238:375—85.
[45] Witten I, Frank E. Data mining: practical machine learning tools and techniques, 2nd ed., San Francisco: Morgan Kaufmann; 2005.
[46] Jang JSR. ANFIS: adaptive network based fuzzy inference systems. IEEE Transactions on System Man and Cybernetics 1993;23(3):665—85.
[47] Shevade SK, Keerthi SS. A simple and efficient algorithm for gene selection using sparse logistic regression. Technical report. CD-02-22, Control Division, Department of Mechanical Engineering, National University of Singapore, Singapore; 2002. p. 117—576.
[48] Liu H, Li J, Wong L. A comparative study on feature selection and classification methods using gene expression profiles and proteomic patterns. Genomic Informatics 2002;13: 51—60.
[49] Timm H, Döring C, Kruse R. Different approaches to fuzzy clustering of incomplete datasets. International Journal of Approximate Reasoning 2004;35:239—49.
[50] Van Cott EM, Laposata M. Coagulation. In: Jacobs DS, et al., editors. The laboratory test handbook. 5th ed., Cleveland: Lexi-Comp; 2001. p. 327—58.
[51] Hoek JA, Sturk A, ten Cate JW, Lamping RJ, Berends F, Borm JJ. Laboratory and clinical evaluation of an assay of thrombin—antithrombin III complexes in plasma. Clinical Chemistry 1988;34:2058—62.
[52] Quah KH, Quek C. MCES: a novel Monte Carlo evaluative selection approach for objective feature selections. IEEE Transactions on Neural Networks 2007;18(2):431—48.
[53] Al-Nafussi A. Ovarian epithelial tumours: common problems in diagnosis. Current Diagnostic Pathology 2004;10:473—99.
[54] Zhang Z, Liu Y, Zhao T. SVM based feature screening applied to hierarchical cervical cancer detection. In: Proceedings of the international conference on diagnostic imaging and analysis; 2002. p. 393—8.
[55] Casillas J, Cordón O, Herrera F. Interpretability improvements to find the balance interpretability—accuracy in fuzzy modeling: an overview. In: Casillas J, Cordón O, Herrera F,

Magdalena L, editors. Accuracy improvements in linguistic fuzzy modeling, Studies in fuzziness and soft computing. Heidelberg: Springer-Verlag; 2003. p. 27—45.
[56] C2I, Centre for Computational Intelligence, http://www.c2i.ntu.edu.sg/; accessed November 28, 2007.
[57] Ang KK, Quek C. RSPOP: rough set-based pseudo-outer-product fuzzy rule identification algorithm. Neural Computation 2005;17(1):205—43.
[58] Liu F, Quek C, Ng GS. A novel generic Hebbian ordering-based fuzzy rule reduction approach to mamdani neuro-fuzzy system. Neural Computation 2007;19(6):1656—80.
[59] Tan TZ, Quek C, Ng GS. Biological brain-inspired genetic complementary learning for stock market and bank failure prediction. Computational Intelligence 2007;23(2):236—61.
[60] Tan TZ, Ng GS, Quek C, Koh SCL. Ovarian cancer prognosis by hemostasis and complementary learning.In: Neural Information Processing, PT 3, Proceedings. Lecture Notes in Computer Science 2006;4234:145—54.
[61] Tung WL, Quek C. FALCON: fuzzy neural control and decision systems using FKP and PFKP clustering algorithms. IEEE Transactions on Systems Man and Cybernetics Part B 2004;34(1):686—94.
[62] Quek C, Tung WL. A novel approach to fuzzy membership functions using the FALCON-MART architecture. Pattern Recognition Letters 2001;22(9):941—58.
[63] Tan TZ, Ng GS, Quek C. A novel biologically and psychologically inspired fuzzy decision support system: hierarchical complementary learning. IEEE Transactions on Computational Biology and Bioinformatics 2008;5(1):67—79.
[64] Tan TZ, Quek C, Ng GS. Chance discovery using complementary learning fuzzy neural network. Studies in Computational Intelligence 2006;30:117—34.